2021 18th International Conference on Electrical Engineering, Computing Science and Automatic Control (CCE). Mexico City, Mexico. November 10-12, 2021

Bandgap dependence on facet and size engineering of TiO_2: A DFT Study

Francisco Javier-Cano
Nanosciences and Nanotechnology Program
CINVESTAV-IPN
Ciudad de México, México
franciscojavier.cano@cinvestav.edu.mx

Araceli Romero-Nuñez
Department of Electrical Engineering (SEES)
CINVESTAV-IPN
Ciudad de México, México
araceli.romero@cinvestav.mx

Anish Jantrania
Department of Biological and Agricultural Engineering
TEXAS A & M UNIVERSITY
Texas, USA
ajantrania@tamu.edu

Hongbo Liu
Instituto Mexicano del Petróleo
Ciudad de México, México
hbliu@imp.mx

A. Kassiba
Institute of Molecular and Materials
Le Mans University
Le Mans, France
kassiba@univ-lemans.fr

S. Velumani
Department of Electrical Engineering (SEES)
CINVESTAV-IPN
Ciudad de México, México
velu@cinvestav.mx

***Abstract*— A theoretical study of different phases, morphologies, and sizes of TiO_2 crystallite is presented. Comparative analysis of structure and properties of anatase, brookite, and rutile phases were performed by XRD, un-modified morphology, and bandgap. Morphology modification of the TiO_2 anatase phase was done by inhibiting the most stable planes, (101) and (011). Optimization of lower bandgap values was refined by varying the crystal volumes of TiO_2 with (101) inhibited planes. Based on the results, a proposal of the best alternative of TiO_2 for visible light activity is proposed considering the phase, inhibition of the growth of specific planes, and crystal size.**

Keywords*—Bandgap, anatase, morphology, photocatalysis, titanium dioxide, DFTB+*

I. Introduction

Titanium dioxide (TiO_2) has several polymorphisms, of which anatase, rutile, and brookite are the naturally growing phases. Both anatase and rutile belong to the same crystal system (tetragonal), while brookite has an orthorhombic crystal structure. For novel applications in solar photocatalysis, the practical application of TiO_2 is inhibited by the low quantum efficiency due to the rapid recombination of the electron-hole pairs and the bandgap energy. Moreover, TiO_2 absorption is achieved in the UV region, which only covers a tiny fraction of the sunlight spectrum (3-5%) [1-3]. Therefore, it is desirable to improve the current properties of TiO_2 to achieve higher photocatalytic efficiency under visible light. Different strategies have been developed to enhance the photocatalytic behavior of titanium dioxide to solve the deficiencies mentioned above. Some common strategies include the incorporation of metals, both on the surface and in the TiO_2 matrix, doping with non-metallic elements, deposition of noble metals, coupling of TiO_2 with other semiconductors, and optimization of the TiO_2 morphology [4,5], being the last option the one studied by the present work.

Morphology of material controls the crystallographic orientation and exposes crystal surfaces that strongly influence their physical and chemical properties [6]. Distinct behaviors have been observed from experiments when exposing certain crystalline planes of TiO_2 [7,8]. Even the toxicity of nanoparticles is dependent on the exposed surfaces; for instance, {001} TiO_2 exhibited higher toxicity to *D. Magna* than {101} TiO_2[9].

While various morphologies have been obtained and characterized experimentally, the more reactive facets are still under debate. How the growth mechanism of those facet-engineered nanostructures results on specific shapes is still unknown [10]. In addition, determining nanomaterials' morphology and exposed faces is critical to an adequate association with performance in specific applications. Theoretical studies facilitate having a perspective on the expected results when modifying the structure of TiO_2; thus, simulation results can be a starting point for the design of appropriate experiments for reproducing materials with desired properties, close to those prior calculated and optimized *in silico*.

In this work, a theoretical study of TiO_2 is presented through DFT calculations using the *BIOVIA Material Studio 2017 software*. Firstly, X-ray diffraction spectra, morphologies, and bandgap were obtained for each of the TiO_2 phases to obtain a compared characterization between them. Subsequently, modification of the TiO_2 anatase structure was made by exposing the most reactive planes on the surface, so (101) and (011) planes were inhibited. Finally, different crystal volumes of TiO_2 with (101) inhibited planes were analyzed, proposing the best alternative of TiO_2 that is active in the visible light range to be used in photocatalytic applications.

978-1-6654-0029-9 / 21 / $ 31.00 © 2021 IEEE

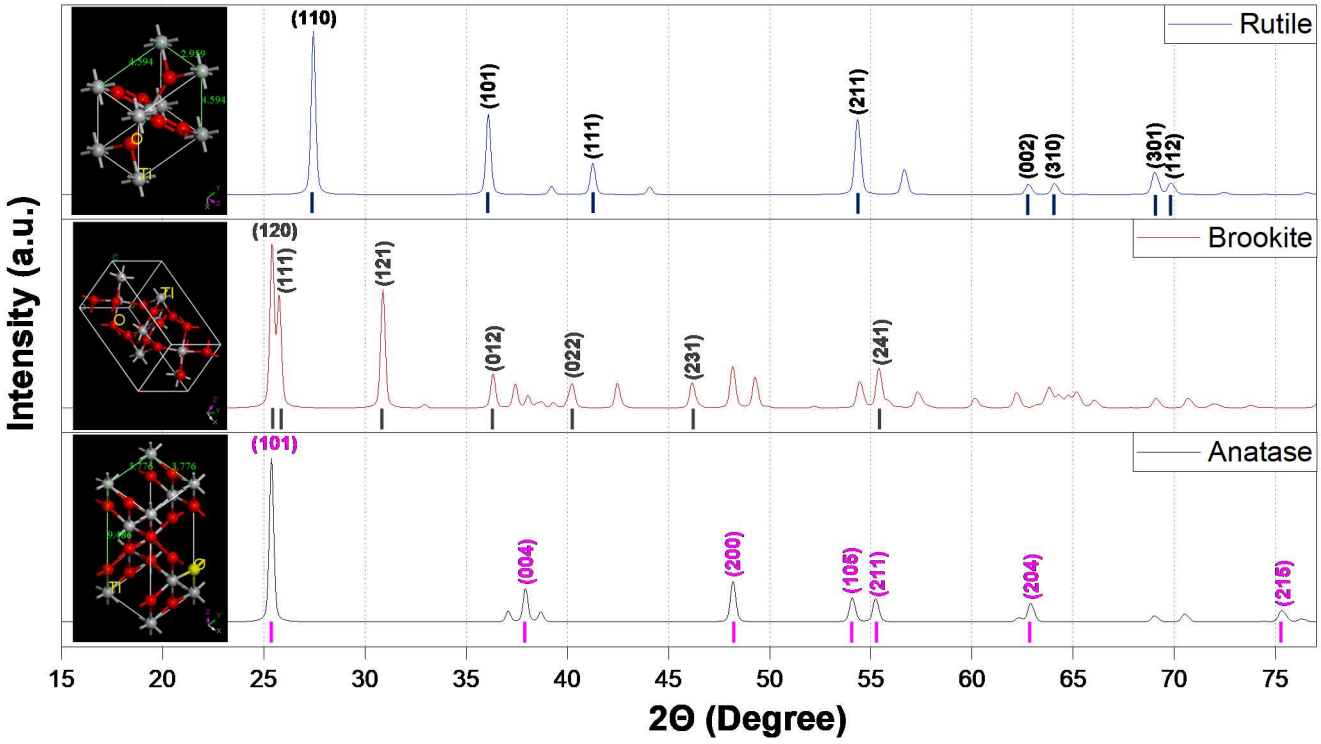

Fig. 1. The equilibrium shape of a TiO_2 crystal in the anatase phase, according to the Wulff construction and surface energies calculated by Lazzeri *et al*. 2001[34].

II. COMPUTATIONAL DETAILS

Structures of the rutile, anatase and brookite phases of TiO_2 were constructed using *BIOVIA Material Studio 2017 Software* based on the structural information of the materials from The Materials Project [11]. As a starting point, the morphology was constructed, and the planes present in each material were identified using the "*Morphology*" module. Thus, the X-ray diffraction patterns (XRD) were obtained using the "*Reflex*" module, where the characteristic peaks for each material were indexed with the "*Powder Indexing*" tool present in the same module. The bandgaps were calculated for each structure using the DFTB+ module. The first step compares the results generated in this work with previous literature; the results proved the modifications of the percentage of planes on the surface of the TiO_2 anatase.

After comparing our resulting phase, the inhibition of planes for TiO_2 anatase was suggested. To the aim, the basic structure of the material was used, and it was cut through the planes (101) and (011), and hence let them grow to different thicknesses, which result in larger structures without the presence of the previously mentioned planes. The tool used for the subsequent procedure was "*build surfaces*". Finally, structures with different dimensions were built, and then their morphologies and bandgap were calculated using the same calculation parameters of the original structures.

III. RESULTS AND DISCUSSION

Figure 1 shows the morphology and X-ray diffraction spectra for different crystalline phases of TiO_2 (Rutile, brookite, and anatase) which were simulated in this work with the help of the "*Morphology*" and "*Reflex*" modules, respectively. Different morphologies are observed for the different phases, so differences between them are easy to observe. The obtained morphologies coincide with the forms of equilibrium for macroscopic crystals previously reported in the literature [12-14]. These morphologies are attributed to the difference in percentages of exposed planes on the surface of each phase. Table I shows the percentage of exposed planes obtained for each crystalline structure simulated in this work.

TABLE I. PERCENTAGE OF PLANES EXPOSED ON THE SURFACE FOR THE TiO_2 PHASES CALCULATED IN THIS WORK.

Phases	**% Main family planes exposed on the surface**			
	{101}	***{110}***	***{001}***	***{111}***
Rutile	40%	59%	--------	-------
Anatase	91.2%	--------	8.8%	-------
Brookite	--------	--------	--------	58%

Equally, the XRD patterns obtained were compared with the standards for each phase: rutile (*JCPDS card nº. 21-1276*), anatase (*JCPDS card nº. 21-1272*), and brookite (*JCPDS card nº. 29-1360*). It is easy to distinguish between anatase and rutile phases since the first two reflection peaks are well separated

(2θ=25.28° for anatase d_{101} vs 2θ=27.44° for rutile d_{110}). Conversely, identifying the difference between anatase and brookite could be more complicated. Alone, the reflection peaks at 2θ=30.81° relating the d_{121} of the brookite phase or at 2θ=62.57° relating d_{204} of the anatase phase can help to make such a difference and/or recognize the presence of both polymorphic forms in an XRD pattern [15]. The bandgap —the energy difference between the valence and conduction bands [16]— for each TiO2 phase is presented in Figure 2. As can be seen, rutile is the phase with the lowest bandgap, with 3.06 eV. In contrast, the highest bandgap was found for the brookite phase, with 3.24 eV, while for the anatase phase, a theoretical bandgap of 3.19 eV was calculated. They are very close to experimental values previously reported in the literature [17-20]. It is observed that the bandgap for all phases is close, so they could all be considered semiconductor materials [21-22]. However, even though the three phases present a close bandgap, according to what has been reported in the literature, only the rutile and anatase phases are catalytically active phases. Among these, anatase has a significant interest because it has shown the highest activity in catalysis and photocatalysis [23]. Compared to anatase, the rutile phase is the least active, properly due to its high recombination rate of electron-hole pairs and its low surface affinity for many organic compounds [4]. Therefore, the anatase phase was chosen for a more specific study, despite having a higher energy band than rutile.

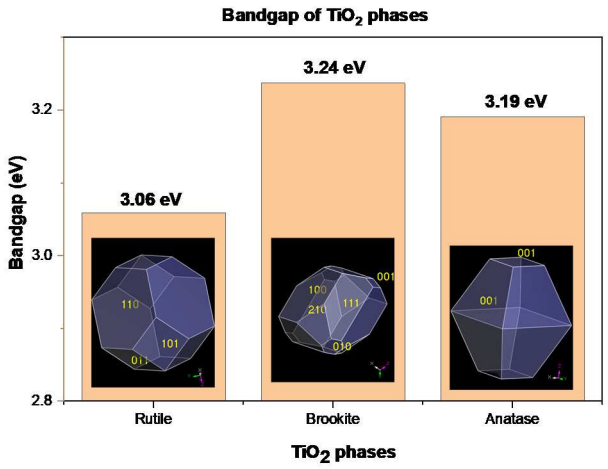

Fig. 2. Bandgap for the different phases of TiO_2.

Generally, anatase TiO_2 has three exposed planes on the surface: (001), (101), and (011) as shown in Figure 3. The average surface energy of anatase TiO_2 reported in the literature is 0.90 $J \cdot m^{-2}$ for {001} and 0.44 $J \cdot m^{-2}$ for {101} [24-28]. Traditionally, TiO_2 anatase crystals are mainly dominated by the {101} planes because they grow spontaneously with the most thermodynamically stable surface, although it is the one with the least reactivity [29,30]. The percentage of {101} planes is 94% in the equilibrium form of the crystals of anatase phase TiO_2 [31]. The simulated morphological results for the phases showed that 91.2% has the {101} family planes while the remaining 8.8% correspond to planes of the family {001}.

The (101) and (011) planes of TiO_2 anatase are more challenging to undergo reduction compared to the plane (001). The difficulty exists because (001) is more efficient at dissociating reactant molecules compared to (101) and (011) due to the low number of exposed atoms coordination, the high density of coordinated unsaturated Ti atoms, and surface oxygen atoms, active with Ti-O-Ti bond angles at (001) [4,32,33]. The origin of this high reactivity appears to be twofold: the high density of uncoordinated Ti atoms on the surface and, probably most important, the tight configuration of atoms on the surface. In addition, there are many angles in the Ti-O-Ti bonds on the surface, indicating *2p* states in highly reactive and destabilized surface oxygen atoms. Therefore, high photocatalytic efficiency is expected for anatase particles with a large percentage of exposed planes {001}[29], although the information regarding its photocatalytic activity is still scarce and sometimes controversial.

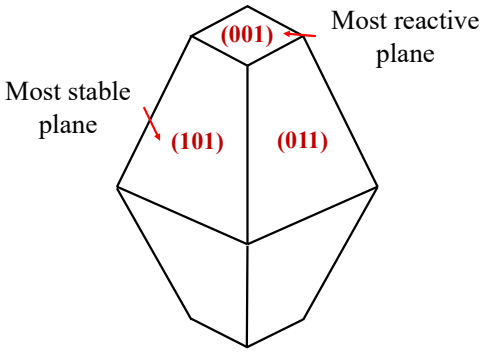

Fig. 3. The equilibrium shape of a TiO_2 crystal in the anatase phase, according to the Wulff construction and surface energies calculated by Lazzeri *et al.* 2001. [34]

For studying the bandgap of the anatase phase, a modification of the original structure of the material was carried out using the inhibition of the planes (101) and (011), respectively. It has been observed that, by inhibiting the growth of certain planes, the growth of others is promoted, causing the morphology and percentage of planes exposed on the surface to change for the original anatase and consequently modifying its electronic properties.

TABLE II. RESULTING PLANES DUE TO PLANES INHIBITION IN ANATASE TiO_2 OBTAINED IN THIS WORK.

Inhibited planes	Resulting planes				Resulting Morphology
	(001)	*(100)*	*(110)*	*(010)*	
(101)	40%	32%	14%	14%	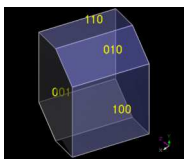
(011)	28%	40%	16%	16%	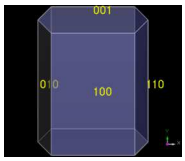

The results showed that by inhibiting the growth of the more stable planes (101) and (011), the growth of the planes (110), (010), (100), and (001) is propitiated. Similar to the original structure, either they were present or in minimal proportion. In both cases, there is a preferential growth of planes (100) and (001), of which, as previously mentioned, (001) is the most reactive plane in the material's structure. By inhibiting the (101) plane, a notable growth of the (001) and (100) planes are observed, representing 40% and 32% of the total surface of the material, respectively. On the other hand, when the inhibited plane is (011), the preferential growth of the plane (100) is observed, being 40% of the surface; while the second plane with the greatest presence is (001), representing the 28% followed by the (110) and (010) planes, with ≈16% of the surface of the material. Table II shows the resulting planes due to plane inhibition.

Figure 4 shows the bandgap calculated for the previously mentioned structures whose planes were inhibited. It is observed that with the inhibition of the planes (101) and (011), a bandgap of 2.34 eV and 2.67 eV are obtained, respectively. In both cases, inhibiting the growth of the most stable planes results in a quite considerable reduction of the bandgap. The advantage allows for constructing TiO_2 anatase structures with enhanced photocatalytic properties in the visible region, even without the need to resort to binary or ternary composites with other materials. Nevertheless, Cushing *et al.,* 2012 [35] mentioned that electron transport between the valence and conduction bands is strongly affected by the crystalline structure and the particle size of the photocatalyst.

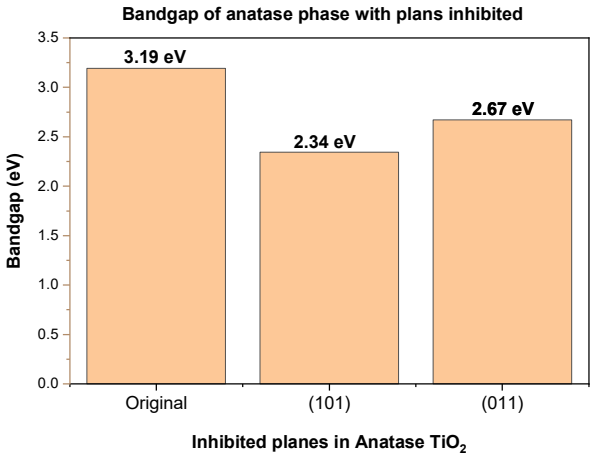

Fig. 4. Bandgap calculated in structures of Anatase TiO_2 with inhibited planes.

Figure 5 shows the gated band behavior calculated for TiO_2 anatase structures with inhibited planes (101) at different volumes. The original anatase has a volume of 136.27 Å^3 [37], however, by inhibiting the most reactive plane (101), the cell volume was reduced to 100.237 Å^3, with a bandgap of 2.343 eV. However, it was observed that upon reaching a volume of 1237 Å^3, the material's bandgap was increased to 2.897 eV; maintaining this value in larger crystal sizes, observing a clear tendency for the bandgap to increase according to the crystal size. It can be said that the critical stage where the best electronic properties of the material are obtained is during the earlier stages of growth, in such a way that these properties are lost until reaching a macroscopic crystal size where they stabilize. The observations were consistent with the results by Lin *et al.,* 2009 [36] that the semiconductor's bandgap energy and other physicochemical properties can change if the particle size decreases or the shape of the nanometric semiconductor particles is modified. In such a way, this represents a strategy to improve the photocatalytic activity of TiO_2 under visible light ($\lambda > 400$ nm), which is equivalent to approximately 43% of the solar irradiation spectrum, which would also allow the use of indoor lighting as a source photoexcitation [38].

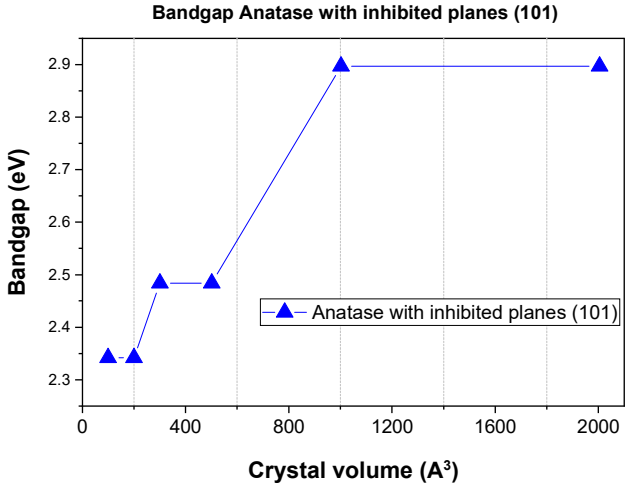

Fig. 5. Bandgap calculated for TiO_2 anatase structures with inhibited planes (101) and different crystal volumes

IV. Conclusion

In this work, the theoretical analysis of the anatase, brookite, and rutile phases of TiO_2 are presented. As expected, our results fully coincide with the results previously reported in the literature, both experimental and theoretical. Of the three simulated phases, the one with the lowest bandgap was the rutile phase. Irrespective of its lower electron-hole recombination rate, it is frequently used in photocatalysis applications in the anatase phase and used for simulation. As a result of the inhibition of the percentage of exposed planes on the TiO_2 surface, it was found that reactive anatase structures, which do not present the most stable planes (101) and (011) on their surface, exhibit a smaller bandgap compared to the original material. Likewise, such results are only presented in small-scale materials, since at larger scales, above ≈500 Å^3, they are lost in a large percentage. The variation of the crystal volume indicates that the material must present nanometric scales, between 100 Å^3 and 500 Å^3, to maintain their light-sensitive performance around 2.4 eV. Larger scales increase bandgap energy.

Acknowledgment

Authors express their gratitude to the Consejo Nacional de Ciencia y Tecnología (CONACYT).

REFERENCES

[1] Sharotri, N., & Sud, D. (2015). *A greener approach to synthesize visible light-responsive nanoporous S-doped TiO_2 with enhanced photocatalytic activity*. New Journal of Chemistry, 39(3), 2217-2223.

[2] Liga, M. V., Bryant, E. L., Colvin, V. L., & Li, Q. (2011). *Virus inactivation by silver doped titanium dioxide nanoparticles for drinking water treatment*. Water Research, 45(2), 535-544.

[3] Xiong, Z., Ma, J., Ng, W. J., Waite, T. D., & Zhao, X. S. (2011). *Silver-modified mesoporous TiO_2 photocatalyst for water purification*. Water research, 45(5), 2095-2103.

[4] Ong, W. J., Tan, L. L., Chai, S. P., Yong, S. T., & Mohamed, A. R. (2014). *Highly reactive {001} facets of TiO_2-based composites: synthesis, formation mechanism and characterization*. Nanoscale, 6(4), 1946-2008.

[5] Kumar, S. G., & Devi, L. G. (2011). *Review on modified TiO_2 photocatalysis under UV/visible light: selected results and related mechanisms on interfacial charge carrier transfer dynamics*. The Journal of physical chemistry A, 115(46), 13211-13241.

[6] Romero-Núñez, A., & Díaz, G. (2015). *High oxygen storage capacity and enhanced catalytic performance of $NiO/Ni_x Ce_{1-x} O_{2-\delta}$ nanorods: synergy between Ni-doping and 1D morphology*. RSC Advances, 5(67), 54571-54579.

[7] Junkaew, A., Ehara, M., Huang, L., & Namuangruk, S. (2021). *Facet-Dependent Catalytic Activity of Anatase TiO_2 for the Selective Catalytic Reduction of NO with NH_3: A Dispersion-Corrected Density Functional Theory Study*. Applied Catalysis A: General, 118250.

[8] Dudziak, S., Kowalkińska, M., Karczewski, J., Pisarek, M., Siuzdak, K., Kubiak, A., ... & Zielińska-Jurek, A. (2021). *Solvothermal growth of {001} exposed anatase nanosheets and their ability to mineralize organic pollutants. The effect of alcohol type and content on the nucleation and growth of TiO_2 nanostructures*. Applied Surface Science, 150360.

[9] Lu, Y., Zhang, H., Wang, H., Ma, N., Sun, T., & Cui, B. (2021). *Humic acid mediated toxicity of faceted TiO_2 nanocrystals to Daphnia magna*. Journal of Hazardous Materials, 416, 126112.

[10] Ma, S., Song, W., Liu, B., Zhong, W., Deng, J., Zheng, H., ... & Zhao, Z. (2016). *Facet-dependent photocatalytic performance of TiO_2: A DFT study*. Applied Catalysis B: Environmental, 198, 1-8.

[11] https://materialsproject.org/

[12] Diebold, U. (2003). *The surface science of titanium dioxide*. Surface science reports, 48(5-8), 53-229.

[13] Gong, X. Q., & Selloni, A. (2007). *First-principles study of the structures and energetics of stoichiometric brookite TiO_2 surfaces*. Physical review B, 76(23), 235307.

[14] Bredow, T., & Jug, K. (1995). *Theoretical investigation of water adsorption at rutile and anatase surfaces*. Surface science, 327(3), 398-408.

[15] Di Paola, A., Bellardita, M., & Palmisano, L. (2013). *Brookite, the least known TiO_2 photocatalyst*. Catalysts, 3(1), 36-73.

[16] Roncali, J. (2007). *Molecular engineering of the bandgap of π-conjugated systems: Facing technological applications*. Macromolecular Rapid Communications, 28(17), 1761-1775.

[17] Amtout, A., & Leonelli, R. (1995). *Optical properties of rutile near its fundamental bandgap*. Physical Review B, 51(11), 6842.

[18] Ekuma, C. E., & Bagayoko, D. (2011). *Ab-initio electronic and structural properties of rutile titanium dioxide*. Japanese Journal of Applied Physics, 50(10R), 101103.

[19] Rocha, I. C. L. (2017). *Síntese solvotérmica de TiO_2 e análise da atividade fotocatalítica*.

[20] Maury, A., & De Belie, N. (2010). *State of the art of TiO_2 containing cementitious materials: self-cleaning properties*. Materiales de construccion, 60(298), 33-50.

[21] Sands, D. E. (1993). *Introduction to crystallography*. Courier Corporation.

[22] Muktavat, K., & Upadhyaya, A. K. (2010). *Applied physics*. IK International Pvt Ltd.

[23] Vittadini, A., Casarin, M., & Selloni, A. (2007). *Chemistry of and on TiO_2-anatase surfaces by DFT calculations: a partial review*. Theoretical Chemistry Accounts, 117(5), 663-671.

[24] Roy, N., Sohn, Y., & Pradhan, D. (2013). *Synergy of low-energy {101} and high-energy {001} TiO_2 crystal facets for enhanced photocatalysis*. ACS nano, 7(3), 2532-2540.

[25] Dai, Y., Cobley, C. M., Zeng, J., Sun, Y., & Xia, Y. (2009). *Synthesis of anatase TiO_2 nanocrystals with exposed {001} facets*. Nano letters, 9(6), 2455-2459.

[26] Pan, J., Wu, X., Wang, L., Liu, G., Lu, G. Q. M., & Cheng, H. M. (2011). *Synthesis of anatase TiO_2 rods with dominant reactive {010} facets for the photoreduction of CO_2 to CH_4 and use in dye-sensitized solar cells*. Chemical Communications, 47(29), 8361-8363.

[27] Wen, C. Z., Jiang, H. B., Qiao, S. Z., Yang, H. G., & Lu, G. Q. M. (2011). *Synthesis of high-reactive facets dominated anatase TiO_2.* Journal of Materials Chemistry, 21(20), 7052-7061.

[28] Wen, C. Z., Zhou, J. Z., Jiang, H. B., Hu, Q. H., Qiao, S. Z., & Yang, H. G. (2011). *Synthesis of micro-sized titanium dioxide nanosheets wholly exposed with high-energy {001} and {100} facets*. Chemical Communications, 47(15), 4400-4402.

[29] Dozzi, M. V., & Selli, E. (2013). *Specific facets-dominated anatase TiO_2: fluorine-mediated synthesis and photoactivity*. Catalysts, 3(2), 455-485.

[30] Yang, H. G., Liu, G., Qiao, S. Z., Sun, C. H., Jin, Y. G., Smith, S. C., ... & Lu, G. Q. (2009). *Solvothermal synthesis and photoreactivity of anatase TiO_2 nanosheets with dominant {001} facets*. Journal of the American Chemical Society, 131(11), 4078-4083.

[31] Liu, G., Jimmy, C. Y., Lu, G. Q. M., & Cheng, H. M. (2011). *Crystal facet engineering of semiconductor photocatalysts: motivations, advances and unique properties*. Chemical Communications, 47(24), 6763-6783.

[32] Chen, W., Kuang, Q., Wang, Q., & Xie, Z. (2015). *Engineering a high energy surface of anatase TiO_2 crystals towards enhanced performance for energy conversion and environmental applications*.

[33] Xu, H., Ouyang, S., Li, P., Kako, T., & Ye, J. (2013). *High-active anatase TiO_2 nanosheets exposed with 95%{100} facets toward efficient H_2 evolution and CO_2 photoreduction*. ACS applied materials & interfaces, 5(4), 1348-1354

[34] Lazzeri, M., Vittadini, A., & Selloni, A. (2001). *Structure and energetics of stoichiometric TiO_2 anatase surfaces*. Physical Review B, 63(15), 155409.

[35] Osterloh, F. E. (2008). *Inorganic materials as catalysts for photochemical splitting of water*. Chemistry of Materials, 20(1), 35-54.

[36] Lin, W. C., Yang, W. D., Huang, I. L., Wu, T. S., & Chung, Z. J. (2009). *Hydrogen Production from Methanol/Water Photocatalytic Decomposition Using $Pt/TiO_{2-x} N_x$ Catalyst*. Energy & Fuels, 23(4), 2192-2196.

[37] Macias B, L. R., Palacios G, J., & Garcia C, R. M. *Quantification of rutile in anatase by means of X-ray diffraction technique.*

[38] Teoh, W. Y., Scott, J. A., & Amal, R. (2012). *Progress in heterogeneous photocatalysis: from classical radical chemistry to engineering nanomaterials and solar reactors*. The Journal of Physical Chemistry Letters, 3(5), 629-639.